Analysis of bioactive oxysterols in newborn mouse brain by LC/MS[s]

Anna Meljon,* Spyridon Theofilopoulos,[†] Cedric H. L. Shackleton,[§] Gordon L. Watson,[§] Norman B. Javitt,** Hans-Joachim Knölker,[††] Ratni Saini,[††] Ernest Arenas,[†] Yuqin Wang,[1,]* and William J. Griffiths[1,]*

Institute of Mass Spectrometry,* College of Medicine, Swansea, UK; Laboratory of Molecular Neurobiology,[†] Department of Medical Biochemistry and Biophysics, Karolinska Institutet, Stockholm, Sweden; Children's Hospital Oakland Research Institute,[§] Oakland, CA; Department of Medicine,** NYU School of Medicine, New York, NY; and Department Chemie,[††] Technische Universität Dresden, Dresden, Germany

Abstract   Unesterified cholesterol is a major component of plasma membranes. In the brain of the adult, it is mostly found in myelin sheaths, where it plays a major architectural role. In the newborn mouse, little myelination of neurons has occurred, and much of this sterol comprises a metabolically active pool. In the current study, we have accessed this metabolically active pool and, using LC/MS, have identified cholesterol precursors and metabolites. Although desmosterol and 24S-hydroxycholesterol represent the major precursor and metabolite, respectively, other steroids, including the oxysterols 22-oxocholesterol, 22R-hydroxycholesterol, 20R, 22R-dihydroxycholesterol, and the C_{21}-neurosteroid progesterone, were identified. 24S,25-epoxycholesterol formed in parallel to cholesterol was also found to be a major sterol in newborn brain. Like 24S- and 22R-hydroxycholesterols, and also desmosterol, 24S,25-epoxycholesterol is a ligand to the liver X receptors, which are expressed in brain.▮▮ The desmosterol metabolites (24Z),26-, (24E),26-, and 7α-hydroxydesmosterol were identified in brain for the first time.—Meljon, A., S. Theofilopoulos, C. H. L. Shackleton, G. L. Watson, N. B. Javitt, H-J. Knölker, R. Saini, E. Arenas, Y. Wang, and W. J. Griffiths. **Analysis of bioactive oxysterols in newborn mouse brain by LC/MS.** *J. Lipid Res.* **2012.** 53: **2469–2483.**

Supplementary key words   sterol • liver X receptor • desmosterol • cholesterol • 24S-hydroxycholesterol • 24S,25-epoxycholesterol • derivatization

In mammals, there are high levels of unesterified cholesterol in brain (10–20 µg/mg wet weight in most species) (1). Cholesterol in brain can be found in three distinct pools: *i*) in the myelin sheaths of oligodendroglia, *ii*) in plasma membranes of neurons and other glial cells, and *iii*) in a metabolically active pool made up of other organelles, e.g., endoplasmic reticulum (ER), Golgi (2, 3). In the newborn mouse, which is born nearly helpless, there is essentially no myelination in the brain, and cholesterol levels in brain are similar to most other organs (2–4 µg/mg). Cholesterol levels subsequently increase rapidly in mouse brain over a three week period during which myelination proceeds (1). Thus, the newborn mouse offers an opportunity to study the sterol content of brain in the absence of masking levels of myelin-derived cholesterol.

Essentially all brain cholesterol is derived from de novo synthesis in brain. This is also true of newborn mouse, where at least 90% of cholesterol in the brain has been synthesized in the brain (4). In the developing fetus, after closure of the blood-brain barrier (BBB), and in the very young animal, desmosterol levels are elevated, indicating a rapid de novo synthesis of sterols (1, 4, 5). An active mevalonate pathway in the developing fetus is further confirmed by appreciable levels of 24S,25-epoxycholesterol (5).

In adult mammals, cholesterol levels in brain are maintained at a constant level and the rate of cholesterol synthesis is equal to that of cholesterol loss. Cholesterol is

---

removed from brain by two mechanisms (6), one of which is metabolism to 24S-hydroxycholesterol, which is able to cross the BBB and is transported via the circulation to the liver for further metabolism (7), and the other has yet to be fully described. In the fetal mouse, the expression of cholesterol 24-hydroxylase (Cyp461a1) is low, possibly to conserve cholesterol (4). However, during the first 2 weeks of life, there is a significant increase in *Cyp46a1* mRNA levels in parallel with an increase in 24S-hydroxycholesterol levels (8, 9).

24S-hydroxycholesterol, like 24S,25-epoxycholesterol, is a ligand in vitro to the liver X receptors (LXRs) (10, 11); this is also true of 22R-hydroxycholesterol. 22R-hydroxycholesterol is an intermediate in the conversion of cholesterol to pregnenolone by the cytochrome P450 (Cyp) side-chain cleavage enzyme (P450$_{SCC}$, Cyp11a1). This enzyme converts cholesterol first to 22R-hydroxycholesterol then to 20R,22R-dihydroxycholesterol, and ultimately to pregnenolone, thus offering a route for neurosteroid biosynthesis (12). 22R-hydroxycholesterol has been reported to be present in human brain and to also have neuroprotective effects in vitro against amyloid β toxicity (13, 14).

Side-chain oxidized sterols can have a regulatory role in cellular cholesterol homeostasis in that they are ligands to Insigs (insulin-induced genes), which, when bound to oxysterols bind to SCAP (SREBP cleavage-activating protein), anchoring the complex in the ER and preventing the transport by SCAP of SREBPs (sterol-regulatory element binding proteins) to the Golgi for processing to their active forms as transcription factors (15). SREBP-2 activates genes encoding the enzymes of the mevalonate pathway required for cholesterol biosynthesis and also for cholesterol uptake (16). Cholesterol can also regulate the processing of SREBPs, but in this case, by binding to SCAP, which triggers binding to Insigs, anchoring SCAP in the ER and preventing transport of SREBPs to the Golgi for processing (17). Current concepts suggest that although cholesterol is the major regulator of its own synthesis, oxysterols have a role in fine-tuning acute cholesterol homeostasis and protecting the cell against over-accumulation of newly synthesized cholesterol (18).

Analysis of sterols, oxysterols, and other steroids in brain can be challenging. This is because of the high level of cholesterol in comparison to that of other steroids and its propensity to undergo autoxidation (19, 20). The major autoxidation products of cholesterol are the oxysterols 7-oxo-, 7β-hydroxy-, 7α-hydroxy-, 25-hydroxy-, 5β, 6β-epoxy-, 5α,6α-epoxy-, and 5α,6β-dihydroxycholesterols, whereas other steroids, e.g., pregnenolone, dehydroepiandrosterone, can also be formed (19, 20). To minimize this problem, many workers utilize butylhydroxytoluene (BHT) as an antioxidant during extraction and/or separation of oxysterols (and neurosteroids) from cholesterol prior to analysis (5, 21–24). MS, coupled with either GC or LC, offers the most-sensitive method of oxysterol and steroid analysis in brain (25). However, GC-MS requires derivatization of oxysterols to avoid thermal decomposition (26), whereas LC-MS, in the absence of derivatization, is usually operated in the multiple reaction monitoring mode to achieve sufficient sensitivity. We and others have exploited derivatization methods in combination with LC-MS to enhance sensitivity (25, 27). Using LC-MS with application of multistage fragmentation (MS^n), we have previously profiled the oxysterol content of adult and embryonic rodent brain (5, 22, 28). We now expand these studies to profile newborn mouse brain.

METHODS

Materials

Sterol, oxysterol, and other steroid standards were obtained from Avanti Polar Lipids (Alabaster, AL), Steraloids, Inc. (Newport, RI), or were synthesized for this and earlier studies (22, 29, 30). The chemical synthesis of cholesta-5,24Z-dien-3β,26-diol and cholesta-5,24E-dien-3β,26-diol will be described elsewhere. Cholesterol oxidase from *Streptomyces* sp. was from Sigma-Aldrich (St. Louis, MO) and Girard P (GP) reagent [1-(carboxymethyl) pyridinium chloride hydrazide] from TCI Europe (Zwijndrecht, Belgium). Solid-phase extraction (SPE) cartridges, Certified Sep-Pak C$_{18}$, 200 mg, were from Waters, Inc. (Elstree, UK). Solvents were from Fisher-Scientific (Loughborough; Leicestershire, UK), water, acetonitrile, methanol, and propan-2-ol were HPLC grade, whereas ethanol was analytical grade. Acetic acid 100% was from VWR International Ltd. (Poole; Dorset, UK), and formic acid 98/100% was from VWR International S.A.S. (Briare, France). Potassium phosphate buffer made from potassium dihydrogen phosphate (KH$_2$PO$_4$) was from Sigma-Aldrich (Japan).

Stock solutions of standard compounds were made by dissolving 1 mg of 24(R/S)-[26,26,26,27,27,27-^{2}H$_6$]hydroxycholesterol, 1 mg of 7-[25,26,26,26,27,27,27-^{2}H$_7$]oxocholesterol, and 10 mg of [25,26,26,26,27,27,27-^{2}H$_7$]cholesterol in 10 ml volumes of propan-2-ol. Ten microliters of the oxysterol stock solutions were diluted with 990 µl of 99.9% ethanol to make working solutions of 1 ng/µl.

Animals

Brain extracts from newborn mice were from Children's Hospital, Oakland Research Institute (USA) and shipped to Swansea (UK) for sterol analysis. All animal work conformed to National Institutes of Health guidelines and was approved by the Institutional Animal Care and Use Committee.

Isolation of sterols/oxysterols from newborn mouse brain

Newborn mouse brain from phenotypically normal animals with a predominant C57BL/6 background (31) was homogenized and extracted in methanol-chloroform (1:1, v/v), and reextracted in methanol. The combined extracts were taken to dryness. The lipid extracts, equivalent of 100 mg of wet tissue, were solubilized in 1.05 ml of 99.9% ethanol containing 50 ng of 24(R/S)-[^{2}H$_6$] hydroxycholesterol and 50 µg of [^{2}H$_7$]cholesterol and ultrasonicated for 15 min at room temperature. Then 0.45 ml of water was added, and the mixture was sonicated for another 15 min. The mixture was centrifuged at 14,000 *g* at 4°C for 60 min, and the supernatant was collected. The extraction procedure was repeated on the lipid residue (with a second 1.05 ml ethanol containing reference standards followed by addition of 0.45 ml water), and the supernatants were combined (final volume 3 ml).

To minimize the possibility of autoxidation of cholesterol during sample preparation, oxysterols were separated from cholesterol in an initial reverse-phase (RP)-SPE step. A Certified Sep-Pak C$_{18}$ (200 mg; Waters) cartridge was washed with 4 ml of 99.9% ethanol followed by an equilibration rinse with 6 ml of 70% ethanol.

The brain extract in 70% ethanol (3 ml) was applied to the cartridge and allowed to flow at a rate of 0.25 ml/min. To aid the flow through the cartridge, a negative pressure was applied to the outlet of the cartridge via a vacuum manifold (Vacuum Processing Station; Agilent, Waghaeusel-Wiesental, Germany). The flow-through was collected. This fraction contains oxysterols (32). A wash with 4 ml 70% ethanol was similarly collected and combined with the flow-through to give fraction SPE1-FR1 (see supplementary Fig. I). The column was washed further with 4 ml of 70% ethanol (SPE1-FR2), and cholesterol was eluted from the cartridge with 2 ml of 99.9% ethanol (SPE1-FR3). A final 2 ml of 99.9% ethanol was applied to the column to elute more hydrophobic sterols from the cartridge (SPE1-FR4). Each fraction was divided into two equal volumes, A and B, and all fractions were dried in a Scanspeed vacuum concentrator (Coolsafe; West Sussex, UK) and reconstituted in 100 µl of propan-2-ol.

An identical procedure was carried out with brains from 15 week young adult female mice.

Oxidation of 3β-hydroxy-5-ene sterols/oxysterols with cholesterol oxidase from *Streptomyces* sp.

Sterols/oxysterols with a 3β-hydroxy-5-ene (or 3β-hydroxy-5α-hydrogen) structure were oxidized to 3-oxo-4-ene (and 3-oxo) analogs with cholesterol oxidase from *Streptomyces* sp. (see supplementary Fig. II) (32, 33). A solution of 1 ml 50 mM phosphate buffer (KH_2PO_4, pH 7) containing 3.0 µl of cholesterol oxidase (2 mg/ml in H_2O, 44 U/mg of protein) was added to the A fractions from above (i.e., SPE1-FR1A → SPE1-FR4A). The mixtures were incubated at 37°C for 1 h, and the reactions were quenched with 2 ml of methanol. The B fractions were treated in an identical fashion but in the absence of cholesterol oxidase and with the 2 ml of added methanol containing 50 ng of 7-[$^2H_7$]oxocholesterol. Cholesterol oxidase from *Streptomyces* sp. is inactive toward lanosterol and 14-*des*methyllanosterol.

Derivatization of 3-oxo-4-ene sterols/oxysterols with Girard P reagent

Neutral sterols/oxysterols are by definition neither acidic nor basic, and are poorly ionized in the atmospheric pressure ionization process; thus, a derivatization method was exploited to enhance their LC-MS analysis (22, 25). Sterols/oxysterols possessing an oxo group (either naturally or via treatment with cholesterol oxidase; see supplementary Fig. II) were derivatized with the GP reagent, which contains a charged quaternary nitrogen (22, 34). To each of the fractions from above (SPE1-FR1A/B → SPE1-FR4A/B), 150 µl of glacial acetic acid and 150 mg of GP hydrazine were added (see supplementary Fig. II). The addition of glacial acetic acid increases the rate of hydrazone formation. The mixture was incubated at room temperature overnight in the dark. We call the combined process of oxidation with cholesterol oxidase and derivatization with GP reagent "charge-tagging."

SPE recycling of sterols/oxysterols

Derivatized sterols/oxysterols were separated from the excess of GP hydrazine by a recycling method (22). Sterol/oxysterol molecules, even when derivatized to the GP hydrazones, are still prone to precipitation in highly aqueous solutions. To tackle this problem, a recycling method was used, where initially, analytes dissolved in 70% methanol were recycled on a second 200 mg Certified Sep-Pak C_{18} cartridge (SPE2). Prior to application of the sample, the column was washed with 6 ml of 100% methanol and 6 ml of 10% methanol before conditioning with 4 ml of 70% methanol. The flow of solvent through the column was aided by a negative pressure applied to the column outlet by a vacuum manifold. The derivatization mixture from

above (∼3 ml, ∼70% methanol) was applied to the column, and effluent was retained. The sample tube was then washed with 1 ml of 70% methanol and applied to the column, followed by a column wash of 1 ml 35% methanol. The effluents were pooled (now ∼5 ml) and diluted with 4 ml of water to give 9 ml of 35% methanol. This solution was then applied to the column, and the flow-through was collected, followed by a wash with 1 ml of 17% methanol. The flow-through and wash were diluted with 9 ml of water to give 19 ml of ∼17% methanol. This solution was again loaded onto the column, followed by a wash with 6 ml of 10% methanol. At this point, all the derivatized sterols/oxysterols were retained on the column whereas excess derivatization reagent was in the 10% methanol wash. Derivatized sterols/oxysterols were then eluted in three separate 1 ml portions of 100% methanol (SPE2-FR1, -FR2, -FR3) followed by 1 ml of 99.9% ethanol (SPE2-FR4). ESI-MS analysis revealed that the derivatized oxysterols were present in the first and second ml of methanol (see supplementary information, Results). Thus, for subsequent analysis of oxysterols, the first two milliliters were combined, whereas for sterol analysis, all three milliliters were combined.

LC-MS and MS^n analysis

The LC-MS(MS^n) system consists of an LTQ-Orbitrap XL (Thermo Fisher Scientific, UK) equipped with an ESI probe, and a Dionex Ultimate 3000 LC system (Dionex, UK). Chromatographic separation was performed using a Hypersil Gold RP column (50 × 2.1 mm, 1.9 µm; Thermo Fisher Scientific) at room temperature. Mobile phase A consisted of 0.1% formic acid in 33.3% methanol, 16.7% acetonitrile. Mobile phase B consisted of 0.1% formic acid in 63.3% methanol, 31.7% acetonitrile. Two different gradients were employed. Gradient 1: After 1 min at 20% B, the proportion of B was raised to 80% B over the next 7 min and maintained at 80% B for further 5 min, before returning to 20% B in 0.1 min. The column was reequilibrated for a further 3.9 min, giving a total run of 17 min. Gradient 2; After 1 min at 20% B, the proportion of B was raised to 55% B over the next 19 min using concave curve gradient (curve 8 according to Chromeleon software). From minute 20, the proportion of B was increased linearly to 80% over 10 min, before returning to 20% B in 0.1 min. The column was reequilibrated for 3.9 min, giving a total run time of 34 min. The longer gradient, Gradient 2, was utilized to enhance the resolution of closely eluting oxysterols but offered reduced throughput and lower sensitivity because peaks became broader. The flow rate for each gradient was 200 µl/min, and the eluent was directed to the ESI source of the LTQ-Orbitrap XL mass spectrometer.

The LTQ-Orbitrap XL mass spectrometer was calibrated using "Cal mix" (Thermo Fisher Scientific) and tuned using GP charge-tagged 19-hydroxycholesterol prior to each analytical session. For subsequent LC-MS and LC-MS^n system tests, GP charge-tagged 19-hydroxycholesterol (1 pg/µl in 60% methanol, 0.1% formic acid) was injected (20 µl) onto the RP column and eluted into the ESI source at a flow-rate of 200 µl/min. The analysis of this reference compound was repeated periodically during the analytical batch (every 10 injections) to ensure mass accuracy and to monitor chromatographic performance. For the analysis of GP charge-tagged sterols/oxysterols from brain, the methanol eluents from the SPE2 fractions were diluted to give solutions of 60% methanol, 0.1% formic acid, 3 pg/µl 24(R/S)-[$^2H_6$] hydroxycholesterol. Twenty microliters of solution was injected onto the LC column (equivalent to 0.06 mg brain). Note that while stable in 100% methanol, the stability of GP-tagged steroids is variable in 60% methanol/0.1% formic acid, and analytes should not be stored in this solution for a prolonged period (>48 h).

The LTQ-Orbitap XL was operated utilizing three scan events. First, a Fourier transform (FT)MS scan in the Orbitrap over the m/z range 400–605 at 30,000 resolution (full width at half-maximum height) was performed, followed by data-dependent MS^2 ($[M]^+\rightarrow$) and MS^3 ($[M]^+\rightarrow[M-79]^+\rightarrow$) events in the linear ion trap (LIT). These MS^n scans in the LIT were performed in parallel to acquisition of the high-resolution MS scan by the Orbitrap. For the MS^2 and MS^3 scans, the precursor-ion isolation width was set at 2 (to select the monoisotopic ion) and the normalized collision energy at 30 and 35 (instrument settings), respectively. A precursor-ion inclusion list was defined according to the m/z of the $[M]^+$ ions of expected sterols/oxysterols so that MS^2 was preferentially performed on these ions in the LIT if their intensity exceeded a preset minimum (500 counts) (see supplementary Table I). If a fragment-ion corresponding to a neutral loss of 79 Da from the precursor-ion was observed in the MS^2 event and was above a minimal signal setting (200 counts), MS^3 was performed on this fragment (see supplementary Fig. III). The general ESI conditions were as follows: spray voltage 5 kV; sheath gas (nitrogen) pressure 25 arbitrary units; auxiliary gas (nitrogen) 5 arbitrary units; ion transfer capillary temperature 300°C; capillary voltage 31 V; tube lens 110 V; and ion polarity positive.

Quantification of sterols/oxysterols

Oxysterols were quantified against 24(R/S)-$[^2H_6]$hydroxycholesterol, whereas sterols were quantified against $[^2H_7]$cholesterol. The quantity of sterols/oxysterols in fractions A represent the sum of sterols/oxysterols oxidized by cholesterol oxidase plus those that naturally contain an oxo group (see supplementary Fig. I). The difference (A−B) represents the quantity of sterols/oxysterols with a 3β-hydroxy group oxidized by cholesterol oxidase to a 3-oxo group, whereas the quantities in B represent sterols/oxysterols with a natural oxo group. Previous studies have shown that once GP-tagged, sterols/oxysterols with a 3-oxo-4-ene structure give a similar response upon analysis by LC-ESI-MS (22). This allows the use of 24(R/S)-$[^2H_6]$hydroxycholesterol and $[^2H_7]$cholesterol as universal internal standards for oxysterols and sterols, respectively.

Recovery experiments

Experiments to evaluate the recovery of different oxysterols were performed by adding known amounts of oxysterol standards (22R-, 24S-, 25-, and (25R),26-hydroxycholesterol) to a portion of homogenized brain. This sample and an equivalent portion of homogenate without added oxysterols were processed and analyzed in parallel. Recovery was calculated as the measured oxysterol level divided by the calculated level.

Luciferase reporter assay

The ability of sterols and oxysterols to activate LXRα and -β was tested in luciferase assays. Transient transfection studies were performed in the mouse substantia nigra-like cell line SN4741. This cell line, which is of neural origin, was selected because the sterols and oxysterols were identified in brain. Cells were plated in 24-well plates (5×10^5 cells/well) 24 h before transfection and transfected with 1 μg of plasmid DNA/well complexed with 2 μl of lipofectamine 2000 (Invitrogen). Cells were transfected with 400 ng of an LXR-responsive luciferase reporter construct, and 200 ng of LXRα or LXRβ. A reporter gene expressing the Renilla luciferase (pRL-TK; Promega) was cotransfected in all experiments as an internal control for normalization of transfection efficiency. After a 12 h incubation, the lipid/DNA mix was replaced with fresh 2.5% serum medium containing vehicle or appropriate ligand (10 μM), as specified in each experiment. Luciferase activities were assayed 24 h later using the Dual-Luciferase Reporter Assay System (Promega), following the manufacturer's protocol.

RESULTS AND DISCUSSION

Oxysterols in brain are accompanied by a 10^3-fold excess of cholesterol (2). Therefore, even a minor degree of autoxidation of cholesterol will significantly alter the oxysterol profile of a sample. Thus, steps should be taken to minimize this possibility. One solution to the problem is to add the antioxidant BHT during sterol/oxysterol extraction and/or perform sample preparation under anaerobic conditions (21, 24). Alternatively, and as performed here, oxysterols are separated from cholesterol at the earliest possible stage of the sample preparation procedure.

During the sample preparation procedure, an oxysterol-rich fraction (SPE1-FR1) was separated from a cholesterol-rich fraction (SPE1-FR3), and both fractions were analyzed in separate LC-MS^n analysis. Oxysterols were eluted with 70% ethanol in fraction 1 from SPE1, i.e., SPE1-FR1, and in their GP-tagged form, in fractions 1 and 2 from SPE2, i.e., SPE2-FR1 and SPE2-FR2 (see supplementary Fig. I). Cholesterol was eluted by 99.9% ethanol in fraction 3 from SPE1 (i.e., SPE1-FR3) and in its derivatized form, in fractions 1, 2 and 3 from the second SPE cartridge (SPE2-FR1, SPE2-FR2, and SPE2-FR3). The elution of the oxysterols and cholesterol in the above fractions was confirmed by monitoring the presence of isotope-labeled 24(R/S)-hydroxycholesterol and cholesterol in each SPE fraction (see supplementary information). The recoveries of the side-chain oxidized sterols, 22R-, 24S-, 25-, and (25R),26-hydroxycholesterol, were found to be in excess of 80%.

Following extraction and GP charge-tagging, the oxysterol and cholesterol fractions from brain were further resolved by RP chromatography, and analytes were identified on the LTQ-Orbitrap XL. The identification of compounds was based on retention time, exact mass, and MS^n fragmentation pattern and comparison with authentic standards. In the absence of authentic standards, presumptive identifications were made based on these data. The availability of authentic standards is noted in supplementary Table II. The FTMS high-resolution scan provides accurate mass (<5 ppm) data, allowing the generation of reconstructed ion chromatograms (RICs) for each m/z value of interest. Subsequent MS^2 ($[M]^+\rightarrow$) and MS^3 ($[M]^+\rightarrow[M-79]^+\rightarrow$) spectra were preferentially recorded on target ions on the include list. MS^3 spectra were recording only on product-ions formed as a result of the neutral loss of 79 Da from $[M]^+$ in the MS^2 event (see supplementary Fig. IIIA). This process provided an additional dimension of separation, inasmuch as the neutral loss of 79 Da is characteristic for GP charge-tagged molecules. Shown in supplementary Fig. IIIA is a schematic displaying the MS^2 fragmentation event in which a precursor ion of m/z 534.4054 (GP-tagged 24S-hydroxycholesterol) gives a neutral loss of 79.0422 Da (loss of pyridine) and a product-ion of m/z 455.3632. When this product-ion is subjected to further fragmentation in MS^3, it gives structurally informative fragment ions. Examples of RICs and specific MS^3 fragmentation patterns from oxysterols isolated from newborn mouse brain are described below.
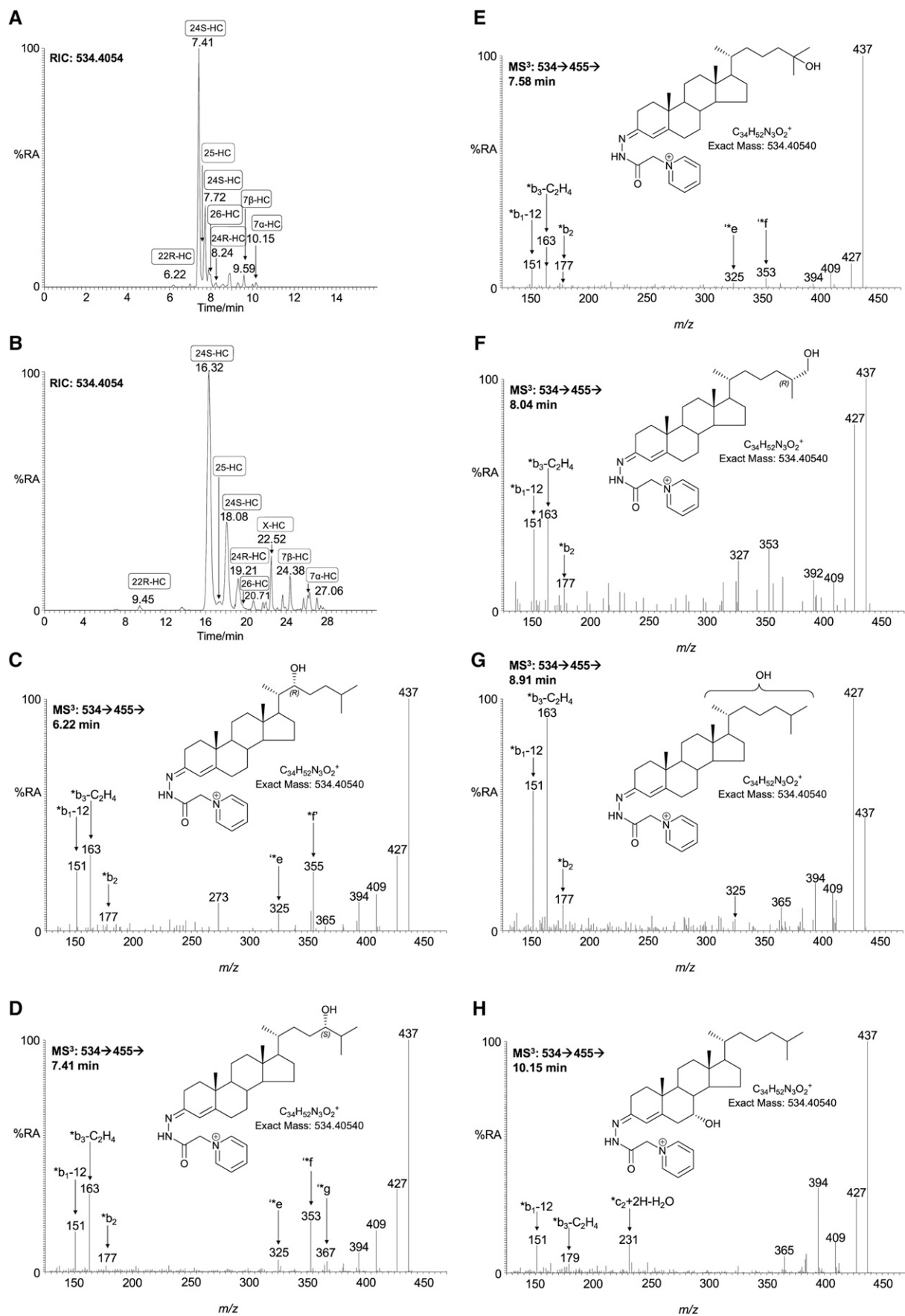
Oxysterols in newborn mouse brain

*Monohydroxycholesterols (*m/z *534.4054).* As in adult mouse brain (9, 21, 24, 25, 35), the most-abundant mono-hydroxycholesterol found in newborn mouse brain is 24S-hydroxycholesterol (**Fig. 1**; supplementary Table II, see also supplementary Table II in (25) and Table III in (36) for published data on adult mouse). Once GP charge-tagged, this oxysterol gives an $[M]^+$ ion of m/z 534.4054. The RIC of this m/z from newborn mouse brain using chromatographic Gradient 1 is shown in **Fig. 2A**. Peaks eluting at 7.41 and 7.72 min are the *syn* and *anti* conformers of GP-tagged 24S-hydroxycholesterol. The MS^3 ($[M]^+ \rightarrow [M-79]^+ \rightarrow$) spectra of both peaks are identical (Fig. 2D) and show the triad of low mass fragment ions m/z 151 (*b_1-12), 163 (*b_3-C_2H_4), and 177 (*b_2) characteristic of the GP-derivatized 3-oxo-4-ene structure (formed following cholesterol oxidase treatment), and a distinctive ion at 353 ('*f'), which is characteristic of the 24-hydroxy group (see supplementary Fig. IIIB) (22). 24S-hydroxycholesterol is generated in the Cyp46a1-catalyzed hydroxylation of cholesterol (8). The Cyp46a1 enzyme is normally expressed in neurons. In newborn mouse brain, the level of 24S-hydroxycholesterol was determined to be 0.510 ± 0.082 ng/mg (mean ± SD, n = 6). This value is considerably lower than that determined here for the young female adult (27.14 ± 1.71 ng/mg, Fig. 1; supplementary Table II) or in the published literature for the adult mouse (30–60 ng/mg) (9, 21, 25, 35). This is not surprising, inasmuch as Cyp46a1 is not expressed until late embryonic development in mouse (4, 9), and in human, Lütjohann et al. (37) have shown that CYP46A1 activity is low in neonates. GP-tagged 24S-, 25-, and 26-hydroxycholesterols (cholest-(25R)-5-ene-3β, 26-diol) give closely eluting peaks but characteristically different MS^3 spectra (Figs. 2D–F). This allows the identification of all three oxysterols. However, in this study, the comparatively high level of 24S-hydroxycholesterol and low levels of the other two closely eluting oxysterols (<0.010 ng/mg) made accurate quantification of the minor oxysterols difficult. Nevertheless, by utilizing the extended chromatographic gradient (Gradient 2), it was possible to
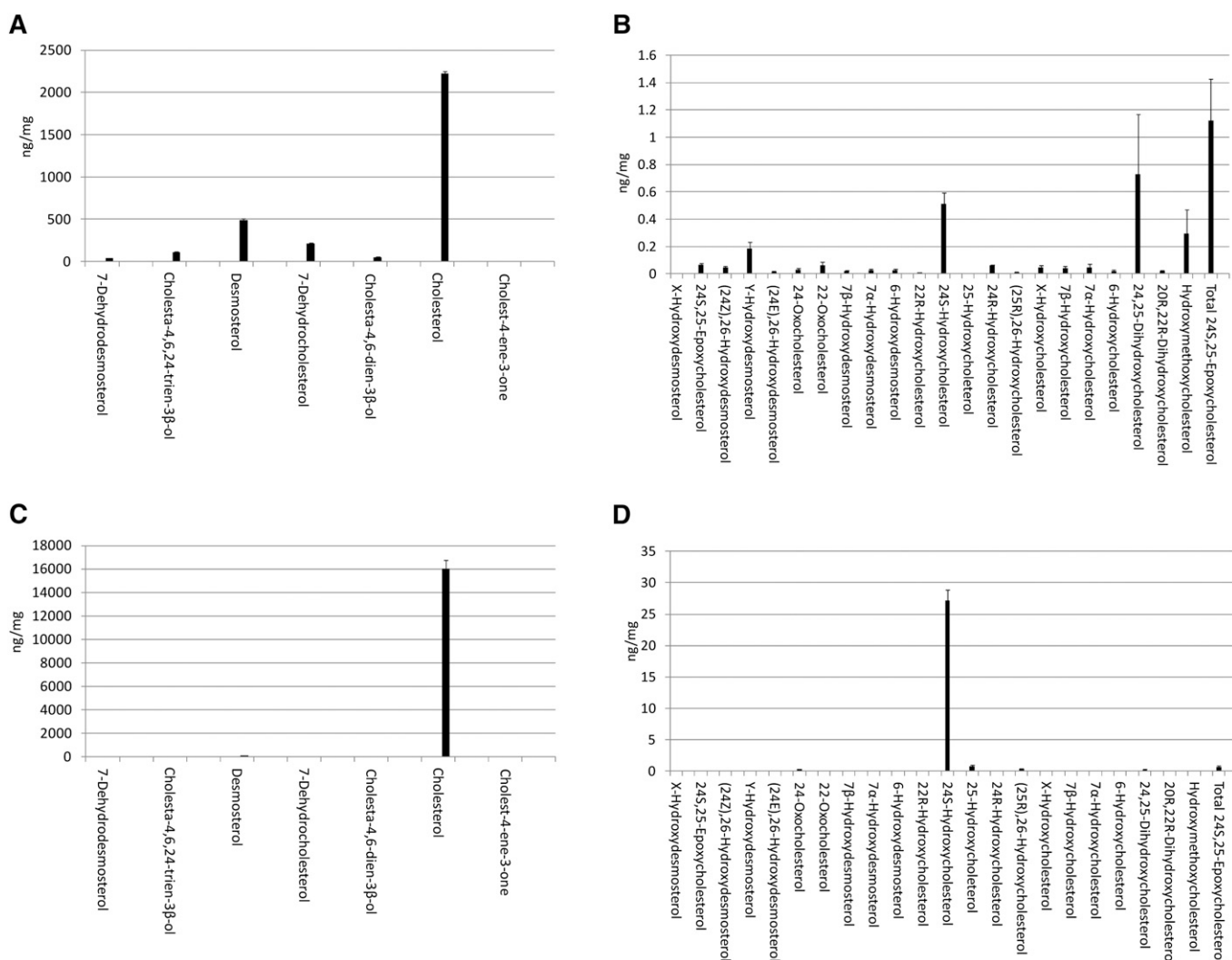
Fig. 1. Sterols and oxysterols in mouse brain. Sterols (A) and oxysterols (B) identified by LC-ESI-MS^n in newborn brain following charge-tagging with GP-hydrazine. In the absence of authentic standards, presumptive identifications based on exact mass, MS^n spectra and retention time are given. Samples from six mice were analyzed. See supplementary Table II for numerical data and further information. Shown in C and D are profiles of sterols and oxysterol, respectively, in 15 week female mouse brain. Data are mean ± SD.

Fig. 2. Monohydroxycholesterols in newborn mouse brain. A, B: RIC of m/z 534.4054 ± 10 ppm utilizing gradients 1 (short) and 2 (long), respectively. C–H: MS^3 ([M]$^+$→[M-79]$^+$→) spectra are assigned to GP-tagged oxysterols. C: 22R-hydroxycholesterol (22R-HC); D: 24S-hydroxycholesterol (24S-HC); E: 25-hydroxycholesterol (25-HC); F: 26-hydroxycholesterol [cholest-(25R)-5-ene-3β,26-diol, 26-HC]; G:

improve the resolution of these isomers and to make quantitative estimates of oxysterol concentrations (Fig. 2B). 25-Hydroxycholesterol is formed from cholesterol either by cholesterol 25-hydroxylase (Ch25h) (38) or in Cyp46a1-catalyzed reactions (8, 39), whereas 26-hydroxycholesterol is formed in Cyp27a1-catalyzed reactions (40, 41). Further scrutiny of the RIC of m/z 534.4054 reveals (Fig. 2A) a minor peak at 8.24 min with retention time and MS^3 spectrum identical to charge-tagged 24R-hydroxycholesterol. Reference to the authentic standard indicates that this compound elutes as *syn* and *anti* conformers, with the earlier eluting component eluting at 7.88 min. These conformers elute at 19.21 and 20.71 min with the longer gradient (Fig. 2B). The level of 24R-hydroxycholesterol was determined to be 0.061 ± 0.006 ng/mg. 24R-hydroxycholesterol has not previously been characterized in brain. In mouse, Cyp46a1 accounts for production of 80% of the 24-hydroxycholesterol content of plasma, and Lund et al. (42, 43) suggested that the remainder may be formed in a reaction catalyzed by Cyp27a1, inasmuch as earlier studies in pig revealed that the hepatic mitochondrial sterol 27-hydroxylase has 24-, 25-, and (25R),26-hydroxylase activity. It is uncertain whether the 24R-isomer found here in newborn brain is formed as a minor product of Cyp46a1 activity in brain or is an import product hepatically derived from Cyp27a1 oxidation of cholesterol. 24R-hydroxycholesterol was not detected in young adult female mouse brain. Preceding the major peaks in the RIC of m/z 534.4054 is a minor peak eluting at 6.22 min (Fig. 2A), identified by retention time and its MS^3 spectrum (Fig. 2C) to correspond to GP-tagged 22R-hydroxycholesterol (0.010 ± 0.002 ng/mg). The presence of a hydroxy group at the C-22 is characterized by an abundant ion at m/z 355 (*f') resulting from a cleavage of the C-20-C-22 bond α to the 22-hydroxy group, and at m/z 273 corresponding to the charge-tagged ABC rings (22). 22R-hydroxycholesterol is formed from cholesterol in the first step of a $P450_{SCC}$ (Cyp11a1) catalyzed reaction and may be further transformed via 20R,22R-dihydroxycholesterol into pregnenolone by the same enzyme. The enzyme is expressed in adult rodent brain and also during embryogenesis (44). Other monohydroxycholesterols identified in newborn mouse brain were 7β-, 7α-, and 6-hydroxycholesterols, at levels of 0.039 ± 0.015, 0.048 ± 0.022, and 0.019 ± 0.014 ng/mg (Fig. 2H). The presence of an additional hydroxy group in the B ring of the steroid nucleus results in a changed pattern of low-mass fragment ions in the MS^3 spectra (see supplementary Fig. IIIC). 7α- or 7β-Hydroxylation causes a shift in the $*b_3-C_2H_4$ ion from m/z 163 to 179. There is an elevated abundance of the ion at m/z 151 ($*b_1$-12) in the spectrum of the 7β-isomer compared with the 7α-isomer, whereas the peaks at m/z 231 and 394 are more pronounced in the spectrum of the 7α isomer. 7α-Hydroxycholesterol can be formed enzymatically in a Cyp7a1-catalyzed reaction, but

Cyp7a1 is expressed only in liver (45). Both 7α- and 7β-hydroxycholesterol can be produced by autoxidation of cholesterol during sample preparation and storage (20), or they may be formed endogenously by reaction of cholesterol with reactive oxygen species (46). In some, but not all samples, a peak giving MS^2 and MS^3 spectra identical to those of the authentic standard of 6β-hydroxycholesterol was observed (see supplementary Table II). 6β-Hydroxycholesterol is a product of 5,6-epoxycholesterol following hydrolysis and dehydration. The remaining chromatographic peak to be characterized corresponds to a hydroxycholesterol eluting at 8.91 min (Fig. 2A) and at 22.52 min (Fig. 2B) (0.045 ± 0.015 ng/mg). The MS^n spectra suggest hydroxylation at a primary or secondary carbon on the C_{17} side-chain (Fig. 2G). One possibility is cholest-(25S)-5-ene-3β,27-diol; however, the retention time does not correspond to that of the authentic standard, which elutes just before the 25R isomer. Note: in this study, we use the nomenclature recommended by lipid maps where 26-hydroxycholesterol corresponds to cholest-(25R)-5-ene-3β,26-diol (47). In summary, the pattern in newborn brain is of one dominating monohydroxycholesterol, i.e., 24S-hydroxycholesterol (Fig. 1). This is similar to that observed here in the young female adult and to published data for adult mouse brain (21, 35). However, it is noteworthy that an array of monohydroxycholesterol isomers are observed in newborn mouse brain, and that a similar situation exists in embryonic brain (5).

Oxo- and epoxycholesterols and hydroxydesmosterols (m/z *532.3898*). Other oxysterols found by Wang et al. (5) to be present in embryonic brain include 24S,25-epoxycholesterol and 24-oxocholesterol, both of which give an $[M]^+$ ion at m/z 532.3898. RICs for this m/z, shown in **Fig. 3A, B**, are generated with the short and long gradient, respectively. The two peaks eluting at RT 6.80 and 7.01 min (Fig. 3A) correspond to the *syn* and *anti* conformers of GP-tagged 24S,25-epoxycholesterol (0.067 ± 0.012 ng/mg). In Fig. 3B, the corresponding peaks are at 12.47 and 13.93 min, respectively. The MS^3 spectra are identical to those of the authentic standard, giving the characteristic low-mass ions at m/z 151, 163, and 177, and side-chain cleavage fragment ions at 325 (*e), 353 (*f), and 367 (*g) (Fig. 3D). The chromatographic peak eluting at 7.79 min (Fig. 3A) was identified as GP-tagged 24-oxocholesterol (0.031 ± 0.008 ng/mg). The presence of a 24-oxo group rather than the 24,25-epoxide is indicated by the elevated abundance of the $[M-79-CO]^+$ ion (m/z 425), compared with the $[M-79-H_2O]^+$ ion (m/z 435) (cf. Fig. 3D, G). 24-Oxocholesterol is an isomerization product of 24S,25-epoxycholesterol formed during the derivatization procedure. Analysis of the newborn mouse brain samples also revealed a peak with a retention time of 8.05 min (Fig. 3A), which gave an MS^3 spectrum characteristic of GP-tagged 22-oxocholesterol (0.060 ± 0.025 ng/mg) (Fig. 3H). Similar to

X-hydroxycholesterol (X-HC); and H: 7α-hydroxycholesterol (7α-HC). Assignment is based on a comparison of retention time, exact mass, and MS^n spectra with those of authentic standards. When charge-tagged with the GP-hydrazone, *syn* and *anti* conformers are formed about the hydrazone group that may or may not be chromatographically resolved. In this study, we use the nomenclature recommended by lipid maps where 26-hydroxycholesterol corresponds to cholest-(25R)-5-ene-3β,26-diol (47).
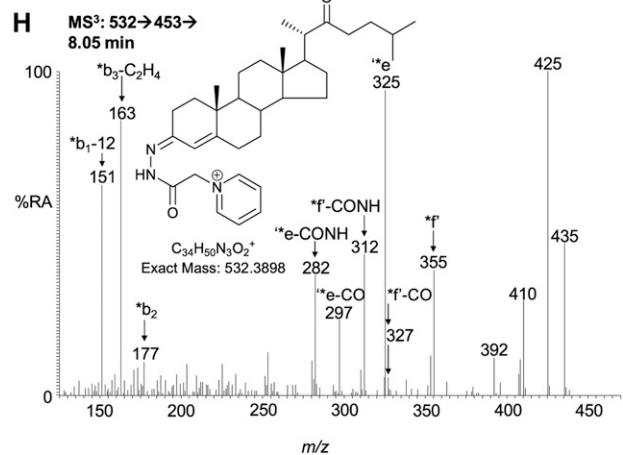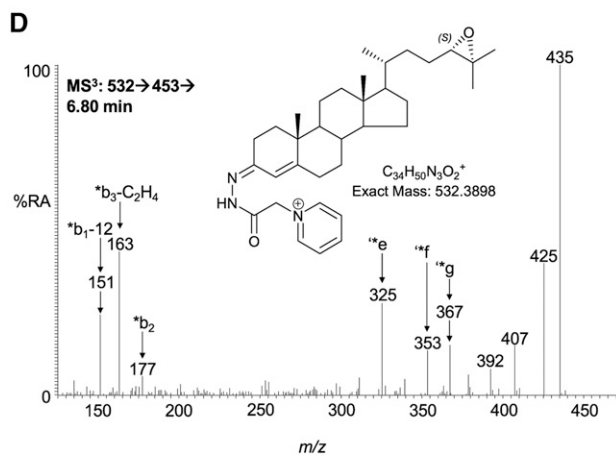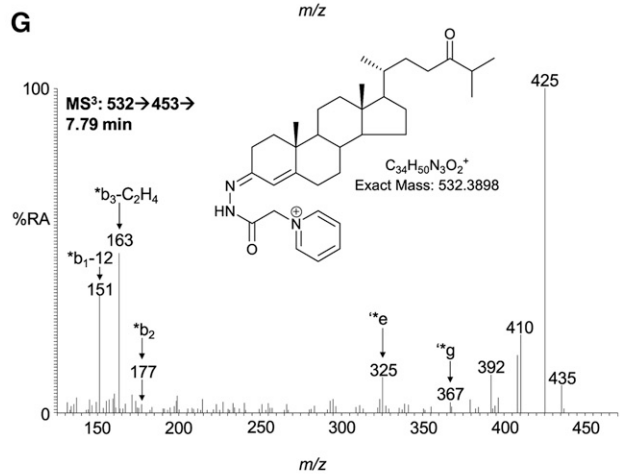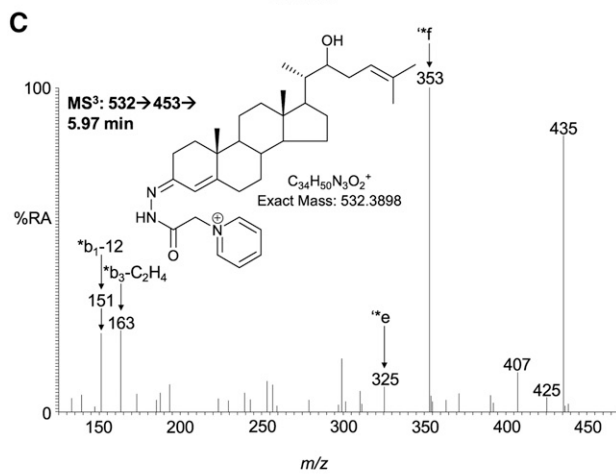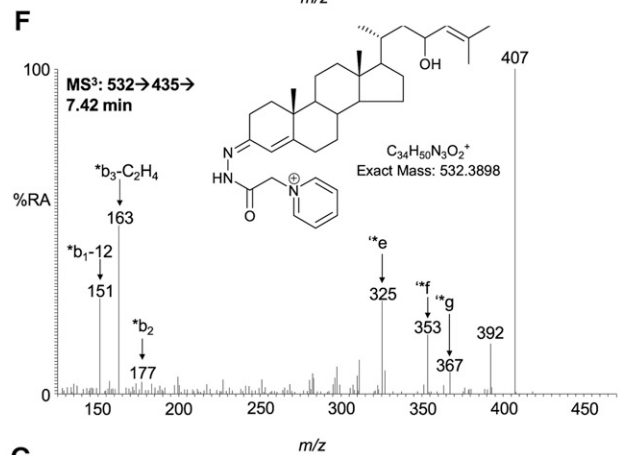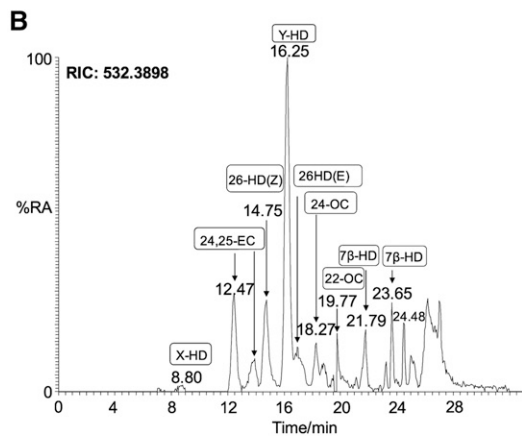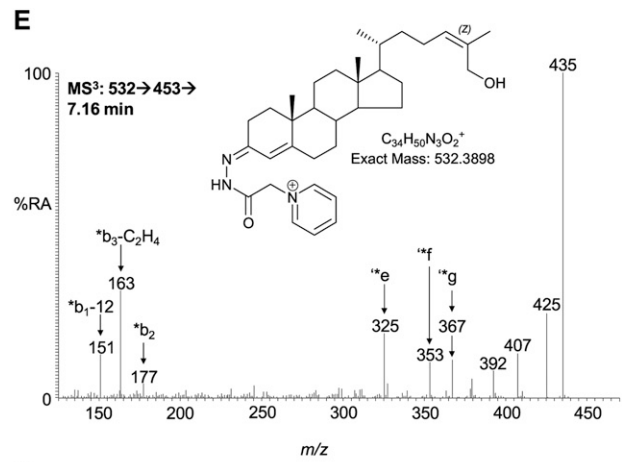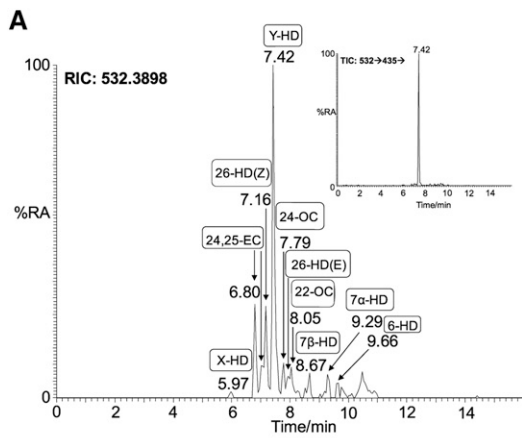
GP-tagged 24-oxocholesterol, the MS^3 spectrum of 22-oxocholesterol shows a major a peak at m/z 425 ([M-79-CO]$^+$); however, the base peak is at m/z 325 ('*e), with satellite peaks at m/z 297 ('*e-CO) and m/z 282 ('*e-CO-NH) (see supplementary Fig. IIID). Other intense peaks are at 355 (*f') and 312 (*f'-CO-NH), in addition to the low-mass triad 151, 163, and 177. The '*e ion at m/z 325 results from cleavage of the C-17-C-20 bond β to the 22-oxo group, probably via a McLafferty-like rearrangement, eliminating the side-chain as an enol (22). The *f' fragment ion results from a cleavage α to the 22-oxo group, with elimination of either a ketene or CO and an alkene (see supplementary Fig. IIID). Further CO and NH moieties are eliminated from the remnants of the derivatizing group to give ions at m/z 327 and 312, respectively. 22-Oxocholesterol has not previously been reported to be present in brain tissue, nor do we find it in the young female adult brain. However, there is a considerable volume of older literature debating its involvement in the side-chain shortening of cholesterol to pregnenolone (48, 49). The dominant peak in the RIC of m/z 532.3898 is at 7.42 min in Fig. 3A and 16.25 min in Fig. 3B (0.188 ± 0.046 ng/mg) and is not easy to assign. The MS^3 ([M]$^+$→[M-79]$^+$→) spectrum is completely dominated by the [M-79-18]$^+$ ion at m/z 435 (see supplementary Fig. IVA). This indicates a facile loss of H_2O from the [M-79]$^+$ ion, possibly to give a thermodynamically stabilized conjugated diene derived from a sterol with hydroxy and alkene groups α,β to one another. The presence of minor ions at m/z 151, 163, 325 ('*e), and 353 ('*f) suggest that the unsaturation and hydroxylation are on the side-chain. By utilizing the MS^n capability of the LIT, it was possible to delve deeper into the structure of the ion of m/z 435. Shown in the inset to Fig. 3A is the total ion chromatogram (TIC) for the [M]$^+$→[M-97]$^+$→ transition. Only one peak is evident, appearing at 7.42 min, and the corresponding MS^3 spectrum is shown in Fig. 3F. The spectrum is compatible with a GP-tagged sterol unsaturated and hydroxylated in the side-chain, possibly 23-hydroxydesmosterol. There is a precedent for C-23 hydroxylation of sterols as part of the 25-hydroxylase pathway to bile acids, but whether this pathway is applicable to desmosterol is unknown (50, 51). Perhaps significantly, an essentially normal bile acid pattern is seen in the cholesterol-free mouse, in which desmosterol is the dominant sterol (52). It should be noted, however, that C-23 is an allylic site in desmosterol and is thus susceptible to nonenzymatic oxidation. An equivalent peak was not observed in the corresponding chromatogram from young adult female brain. The partial identification of a hydroxylated desmosterol encouraged us to search for further isomers of this molecule. Pikuleva

and Javitt (30) have shown that desmosterol can be 26-hydroxylated by human recombinant CYP27A1, whereas Heverin et al. (52) have identified this oxysterol in the cholesterol-free mouse. The retention time of an authentic charge-tagged (24Z),26-hydroxydesmosterol (cholesta-5, 24Z-diene-3β,26-diol) run with the short gradient is 7.16 min, and a peak appearing in the RIC of m/z 532.3898 at this retention time (0.048 ± 0.009 ng/mg) gives a spectrum essentially identical to that of the authentic standard (Fig. 3E). By utilizing the extended chromatographic gradient (24Z), 26-hydroxydesmosterol was completely resolved from the second peak of 24S,25-epoxycholesterol (cf. Fig. 3A, B). Hydroxylation of the terminal carbon of desmosterol introduces Z or E stereochemistry about the C-24-25 double bond, and these isomers are readily resolved by utilizing the extended gradient, allowing the identification also of (24E),26-hydroxydesmosterol (cholesta-5, 24E-diene-3β,26-diol) eluting at 16.85 min in the chromatogram of newborn brain (0.015 ± 0.004 ng/mg; supplementary Fig. IVB). A minor peak is seen (Fig. 3A) at 5.97 min, and the MS^3 spectrum (Fig. 3C) is again compatible with a GP-tagged hydroxydesmosterol, with an added hydroxy group on the side-chain (0.002 ± 0.002 ng/mg). Further inspection of the RIC of m/z 532.3898 (Fig. 3A) reveals peaks at 8.67 and 9.29 that give MS^3 spectra compatible with GP-tagged 7β- and 7α-hydroxydesmosterols, respectively (0.020 ± 0.006 and 0.024 ± 0.012 ng/mg) (see supplementary Fig. IVC, D). The 7α isomer is probably formed, at least in part, endogenously in a Cyp-catalyzed hydroxylation of desmosterol. Cyp7a1 has activity toward desmosterol, although 7α-hydroxydesmosterol was not found in plasma of the cholesterol-free mouse (52). A peak at 9.66 min (Fig. 3A) gives an MS^3 spectrum commensurate with a GP-tagged 6-hydroxydesmosterol (0.023 ± 0.011 ng/mg), probably derived from 5,6-epoxydesmosterol (see supplementary Fig. IVE). The hydroxydesmosterol molecules described here have not previously been found in brain, and of the isomers characterized, only (24Z),26-hydroxydesmosterol is found in the young adult.

Dihydroxycholesterols (m/z 550.4003). The chromatogram of GP-tagged dihydroxycholesterols (m/z 550.4003; **Fig. 4A**), acquired using the short gradient, revealed two major peaks eluting at 3.95 min and 4.62 min, identified as the *syn* and *anti* conformers of GP-tagged 24, 25-dihydroxycholesterol (0.731 ± 0.439 ng/mg) (Fig. 4B). The MS^3 spectra shows features characteristic of hydroxylation at C-24 and C-25, i.e., m/z 325 ('*e), 353 ('*f), 367 ('*g), and 381 ('*h). The presence of hydroxylation at C-25 is further reflected by the dominating [M-79-H_2O]$^+$

Fig. 3. Oxo and epoxycholesterols and hydroxydesmosterols in newborn mouse brain. RIC of m/z 532.3898 ± 10 ppm acquired using the short (A) and long (B) gradient. The inset in A shows the TIC for the [M]$^+$→[M-97]$^+$→ transition. C–E, G–H: MS^3 ([M]$^+$→[M-79]$^+$→), and F: [M]$^+$→[M-97]$^+$→ spectra are assigned to GP-tagged oxysterols. C: X-hydroxydesmosterol (X-HD); D: 24S,25-epoxycholesterol (24,25-EC); E: (24Z),26-hydroxydesmosterol [cholesta-5,24Z-diene-3β,26-diol, 26-HD(24Z)]; F: Y-hydroxydesmosterol (Y-HD); G: 24-oxocholesterol (24-OC); H: 22-oxocholesterol (22-OC). Assignments are based on a comparison of retention time, exact mass, and MS^n spectra with, where possible, those of authentic standards. Authentic standards were available for 24S,25-epoxycholesterol, (24Z),26-hydroxydesmosterol, (24E),26-hydroxydesmosterol, 24-oxocholesterol, and 22-oxocholesterol. X and Y correspond to locations of hydroxy groups on the C-17 side-chain, probably at C-22 and -23, respectively.
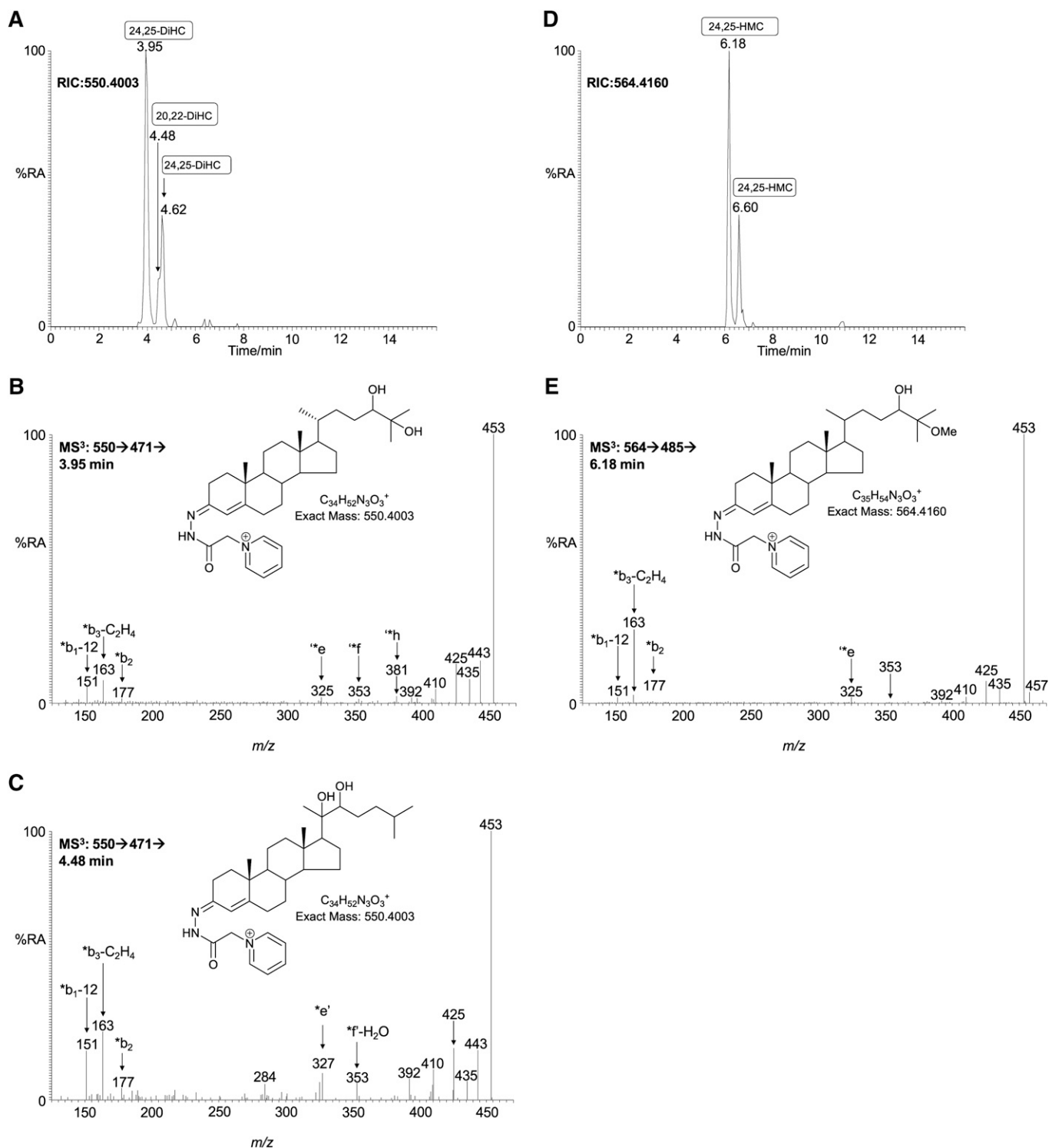
Fig. 4. Dihydroxycholesterols and hydroxymethoxycholesterols in newborn mouse brain. A: RIC of m/z 550.4003 ± 10 ppm acquired with the short gradient. MS^3 ($[M]^+ \rightarrow [M-79]^+ \rightarrow$) spectra are assigned to GP-tagged (B) 24,25-dihydroxycholesterol (24,25-DiHC) and (C) 20R,22R-dihydroxycholesterol (20,22-DiHC). D: RIC of m/z 564.4160 ± 10 ppm generated using the short gradient. E: MS^3 ($[M]^+ \rightarrow [M-79]^+ \rightarrow$) spectrum assigned to GP-tagged 24-hydroxy-25-methoxycholesterol (or the 25-hydroxy-24-methoxy isomer, 24,25-HMC). Assignment is based on retention time, exact mass, and MS^n spectra in comparison with authentic standards. 24,25-Dihydroxycholesterol and 24-hydroxy-25-methoxycholesterol are hydrolysis and methanolysis products of 24S,25-epoxycholesterol. When the derivatization is carried out in ethanol, the corresponding ethanolysis product is identified. The MS^3 spectrum assigned to 20R,22R-dihydroxycholesterol is distorted to some extent by partial overlap with 24,25-dihydroxycholesterol. Nevertheless, the characteristic pattern of ions at m/z 284 (*e'-CO-NH), 297 (*e-CO*), and 325/327 ('*e/*e') is evident.

ion at m/z 453. 24,25-Dihydroxycholesterol can he formed by hydrolysis of chemically labile 24S,25-epoxycholesterol. The acidic methanolic environment of derivatization can also cause methanolysis of 24S,25-epoxycholesterol, leading to formation of hydroxymethoxycholesterol isomers (0.294 ± 0.177 ng/mg) (Fig. 4D). Analysis of the RIC of m/z 564.4160 (Fig. 4D) showed two peaks with retention times and MS^3 fragmentation profiles identical to those obtained during the analysis of the GP-tagged reference standard (Fig. 4E). The $[M-79-32]^+$ ion (m/z 453) is characteristic of the presence of a methoxy group that eliminates as methanol. The combined concentration of 24S,25-epoxycholesterol (0.067 ng/mg), 24-oxocholesterol (0.031 ng/mg), 24,25-dihydroxycholesterol (0.731 ng/mg), and hydroxymethoxycholesterol (0.294 ng/mg) equals 1.123 ± 0.304 ng/mg. 24S,25-Epoxycholesterol is formed in a shunt of the mevalonate pathway, so the comparatively high level of this oxysterol is not unexpected for a developing tissue with high rate of cholesterol synthesis (1). For comparison, the level of 24S,25-epoxycholesterol is only 0.64 ng/mg in the young adult female mouse. Close inspection of the RIC for m/z 550.4003 (Fig. 4A) reveals a shoulder (4.48 min) on the leading edge of the peak at 4.62 min. This is partially resolved with the longer gradient (see supplementary Fig. VA) The MS^3 spectrum recorded suggests the presence of 20R,22R-dihydroxycholesterol (0.020 ± 0.007 ng/mg) (Fig. 4C) providing the first direct evidence for the presence of this cholesterol metabolite in brain. 20R,22R-Dihydroxycholesterol is an intermediate in the conversion of cholesterol to pregnenolone. Its presence in newborn brain lends weight to the argument that neurosteroids are formed in brain, rather than just passengers from the circulation (12).
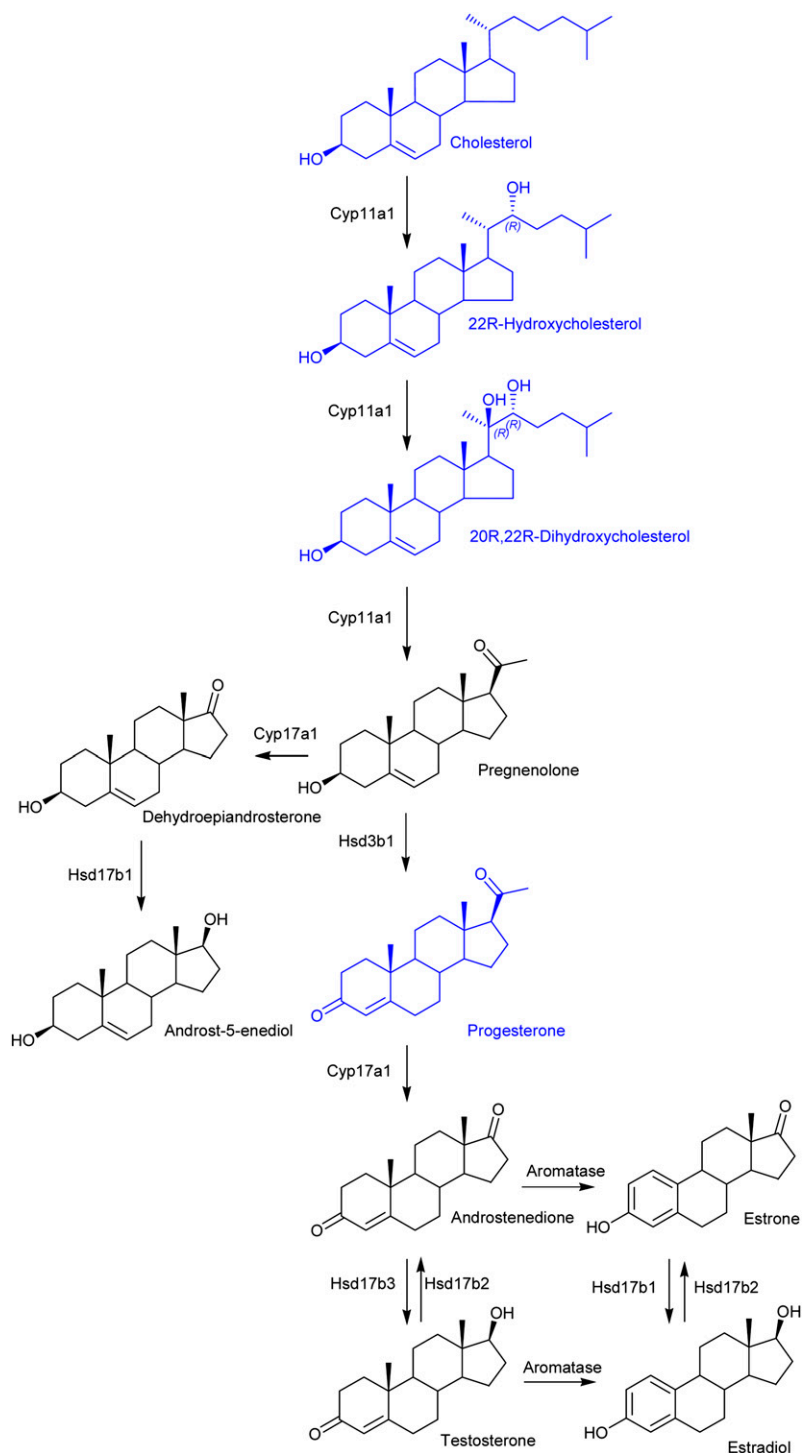
Neurosteroids in newborn mouse brain

Because we are able to identify both 22R-hydroxycholesterol and 20R,22R-dihydroxycholesterol in brain, the possibility exists that neurosteroidogenesis is proceeding in brain (**Fig. 5**). Although we failed to identify pregnenolone, progesterone was conclusively identified (0.001 ± 0.001 ng/mg) (see supplementary Fig. VI). Liu, Sjövall, and Griffiths (23) also found progesterone to be the most-abundant neurosteroid in adult rodent brain (0.001–0.020 ng/mg).

Sterols in newborn mouse brain

Cholesterol and its precursors desmosterol (Bloch pathway) and 7-dehydrocholesterol (Kandutsch-Russell pathway) elute from the first SPE column in fraction 3 (SPE1-FR3). Following GP charge tagging, this fraction was also analyzed by LC-MS. Due to the high concentration of cholesterol, it was necessary to dilute the eluent from the second SPE column by a factor of 10,000–20,000 prior to injection on the LC-MS system. The RIC of m/z 518.4105 corresponding to GP charge-tagged cholesterol is shown in supplementary Fig. VIIA. The major component elutes at 12.83 min and gives an MS^3 spectrum identical to that of GP-tagged cholesterol (see supplementary Fig. VIIB). The concentration of cholesterol in newborn brain was calculated to be 2.221 ± 0.032 µg/mg. Using GC-MS, Marcos et al. (31)

determined a similar value for 1 day-old animals. These values compare with levels in the young female adult, determined here to be 16.026 ± 0.758 µg/mg, and with literature values for the adult of 10–20 µg/mg (9, 21, 31, 35). Cholest-4-en-3-one is also present in newborn brain, but at a level of about 0.1% that of cholesterol. Lathosterol is an isomer of cholesterol and a precursor in the Kandutsch-Russell pathway. Like cholesterol, it gives an $[M]^+$ ion of m/z 518.4105. The dynamic range of our LC-MS system is insufficient to observe this isomer against the dominating background of cholesterol. Others have also experienced similar problems using LC-MS for the analysis of sterols in plasma (53). The RIC for m/z 516.3948, corresponding in m/z to GP-tagged desmosterol and 7-dehydrocholesterol, revealed one major peak, with a second appearing as a doublet (see supplementary Fig. VIIIA). The first peak, eluting at 11.33 min, corresponds to GP-tagged desmosterol (493.986 ± 18.062 ng/mg) (see supplementary Fig. VIIIB). This corresponds to about 20% of the total sterol content of newborn brain and agrees well with the value determined by Tint et al. (4) for a 22day fetus. Tint et al. also showed that in the fetus and newborn animal, the expression of 24-dehydrocholesterol reductase (*Dhcr24*) in brain is low, explaining the high level of desmosterol. For comparison, in the young female adult, the desmosterol proportion of total sterols is less than 1%. The first component of the second peak, eluting at 12.07, gives an MS^3 spectrum identical to that of GP-tagged 7-dehydrocholesterol (see supplementary Fig. VIIIC). The second component, at 12.28 min, gives an MS^3 spectrum that we identify as cholesta-4,6-dien-3β-ol. This may be an isomerization product of 7-dehydrocholesterol. Each analyte is present at high concentrations in newborn brain, i.e., 210.484 ± 8.319 ng/mg, and 46.692 ± 6.736 ng/mg, respectively. The prevalence of cholesterol precursors indicates a high rate of cholesterol synthesis during neonatal development and is in good agreement with earlier reports showing that in the developing fetus and suckling newborn, the rates of sterol accumulation in brain are greatest (54). Quan et al. (54) measured both desmosterol and cholesterol levels in the central nervous system of mice, and at their earliest time point of 2 days old, desmosterol made up 30% of total sterols, whereas at day 15, desmosterol had "essentially disappeared." The high levels of desmosterol in the newborn animal are particularly interesting in light of recent data indicating that desmosterol can suppress SREBP processing and activate LXR target genes (55, 56). The precursor of desmosterol is 7-dehydrodesmosterol. A component eluting at 10.85 min in the RIC for m/z 514.3792 (see supplementary Fig. IXA) gives an MS^3 spectrum commensurate with that expected for GP-tagged 7-dehydrodesmosterol (41.159 ± 2.503 ng/mg), and a later-eluting peak at 11.59 min is assigned to cholesta-4,6,24-trien-3β-ol (113.33 ± 7.018) (see supplementary Fig. IX). This may be an isomerization product of 7-dehydrodesmosterol. Again, a high level of cholesterol precursors in newborn brain can be explained by a low expression of *Dhcr24*.

A disadvantage of the analytical method employed in the present study is the laborious requirement to work up

Fig. 5. Neurosteroidogenesis in newborn mouse brain. Shown in blue are sterols, oxysterols, and steroids identified in the present study. Enzymes needed to effect the transitions are indicated.

each brain sample in duplicate, i.e., with and without the addition of cholesterol oxidase (see supplementary Fig. I). In the absence of cholesterol oxidase, only sterols/oxysterols with a natural oxo group will be detected, inasmuch as cholesterol oxidase is required for the detection of sterols/oxysterols with a 3β-hydroxy-5-ene function. A further disadvantage is that cholesterol oxidase from *Streptomyces* sp. is inactive toward lanosterol and 14-*des*methyllanosterol (33), presumably because of the two methyl groups on C-4; so these two molecules are transparent to analysis. It is worth noting that Roberg-Larsen et al. (57) have now developed an automated SPE-LC-MS/MS method for analysis of oxysterols derivatized with the GP reagent.

Sterols and oxysterols as LXR ligands

Many of the sterols and oxysterols identified above have previously been tested for their activation capacity toward nuclear receptors (10, 11, 56). Here we compliment earlier work by testing the activity of desmosterol, the chemically synthesized 24Z and 24E isomers of 26-hydroxydesmosterol, and the structural isomers 24- and 22-oxocholesterol in a cell line of neural origin (**Fig. 6**).
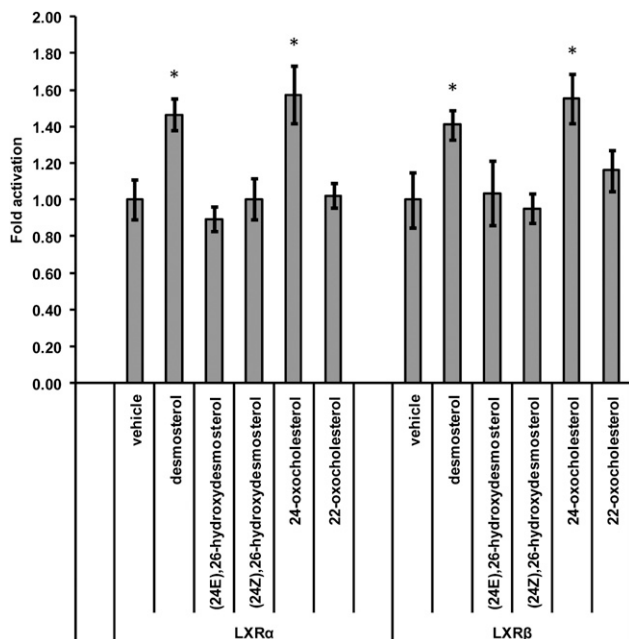
Fig. 6. Analysis of the nuclear receptor activational capacity of sterols and oxysterols. Analysis of luciferase activity in SN4741 cells (mouse neuronal cell line) transfected with an LXR-responsive luciferase reporter construct (LXRE) and LXRα or -β and stimulated for 24 h with desmosterol (10 μm) or the compounds indicated, all at 10 μM, i.e., (24E),26-hydroxydesmosterol; (24Z),26-hydroxydesmosterol; 24-oxocholesterol; and 22-oxocholesterol. The firefly luciferase activity was normalized to Renilla luciferase activity, and the values are expressed as fold activation over the normalized basal LXR response element-luciferase activity set to 1. Data are means ± SE (n = 3); *$P < 0.05$, compared with vehicle treatment.

Luciferase assays were performed in the mouse substancia nigra-like cell line SN4741. Both LXRα and -β have been shown to be expressed in developing brain (58, 59), and we have previously shown 24S,25-epoxycholesterol, 22R-, 24S-, and 25-hydroxycholesterols to be LXR ligands in this cell line (32, 58). 26-Hydroxycholesterol was not found to be an LXR ligand in this cell line. In the current study, we have extended our earlier work and show that desmosterol is an LXR ligand in SN4741 cells, but neither of the 26-hydroxydesmosterol isomers are ligands. Of the two oxo compounds tested, only 24-oxocholesterol was found to be an LXR ligand. However, this is derived from 24S,25-epoxycholesterol during our derivatization reaction. Admittedly, in this cell line, the response to LXR activation by desmosterol is rather low, but it is found to be statistically significant and reproducible. To confirm the results of the luciferase assay, immunoblot analysis was performed against ABCA1, an LXR target protein (see supplementary information). Both 24-oxocholesterol and desmosterol increased the level of ABCA1 in SN4741 cells (see supplementary Fig. X). Although the 10 μM concentration of ligand used is high, the level of desmosterol in newborn brain of ~500 ng/mg suggests that high concentrations could be reached at specific locations.

CONCLUSIONS

There are three major findings of the current study. First, we detect the C_{21}-neurosteroid progesterone and its biosynthetic precursors 22R-hydroxycholesterol and 20R,22R-dihydroxcholesterol in newborn brain (Fig. 5). Second, we find high levels of the LXR and Insig ligand 24S,25-epoxycholesterol in newborn brain (Fig. 1B), and third, we identify numerous oxysterols derived from desmosterol. We also find that desmosterol, but not its 26-hydroxy metabolites, is a ligand to LXR in neural cells (Fig. 6). Furthermore, this is the first identification of the (24Z),26-hydroxydesmosterol isomer in a biological system. These findings have been made utilizing a "charge-tagging" approach for oxysterol/sterol LC-MS(MS^n) analysis, which offers high sensitivity and allows structural characterizations.

In recent years, there has been some controversy over whether and to what extent neurosteroidogenosis proceeds in brain (12, 19, 23, 60). Neurosteroids are C_{18}–C_{21} steroids synthesized in brain. In general, they mediate their actions not through classical steroid hormone (nuclear) receptors, but via ion-gated neurotransmitter receptors, in which case they are called neuroactive steroids. Recent data have also implicated neurosteroids with the inflammatory response in brain, but in this case, via selective modulation of the estrogen receptor β (61). It is often unclear whether a steroid found in brain is synthesized in the brain itself or imported from the circulation. Data presented here, confirming the presence of intermediates of a neurosteroid biosynthetic pathway in developing mouse brain, lends weight to the neurosteroid hypothesis. However, it should be noted that detection of a steroid in situ does not necessarily equate to its synthesis in situ. The present study was not designed to specifically analyze neurosteroids; however, this could be achieved by minor modification to the sample isolation procedure (23), and to the charge-tagging procedure by using cholesterol oxidase from *Brevibacterium*, which also catalyzes the oxidation of 3β-hydroxy-5-ene steroids of the C_{19} and C_{21} series, rather than from *Streptomyces*, which prefers a longer steroid side-chain (33), and by loading greater quantities of sample on the LC column.

In earlier studies, we have shown that embryonic mouse brain contains appreciable amounts of 24S,25-epoxycholesterol (0.1–0.4 ng/mg at E11.5), confirming an active mevalonate pathway during brain development (5). Interestingly, at E11.5, the levels of 24S,25-epoxycholesterol exceed those of the oxysterols enzymatically derived from cholesterol (<0.1 ng/mg) (5). A similar picture is seen here in newborn brain, in which the 24S,25-epoxycholesterol levels (1.123 ± 0.304 ng/mg) exceed other oxysterols, including 24S-hydroxycholesterol (0.510 ± 0.082 ng/mg) (Fig. 1B), the most-abundant oxysterol found in the adult. In the newborn animal, a wide range of oxysterols are identified in brain (Fig. 1B; see supplementary Table II). This is also true in embryonic brain (5), but not in the adult, probably because of the predominance of 24S-hydroxycholesterol, which tends to obscure the observation

of other oxysterols present at low levels. The explanation for the high 24S,25-epoxycholesterol-to-24S-hydroxycholesterol ratio in embryonic and newborn brain compared with the adult is likely to be multifactorial, but reflects a high flow of metabolites through the mevalonate pathway, including the shunt pathway, in the developing brain, and a much-reduced flow rate in the adult (1, 3). Furthermore, the low expression of *Dhcr24* in the embryo and newborn animal (4) may divert sterol biosynthesis from the Bloch and Kandutsch-Russell pathways to the shunt pathway, which does not utilize *Dhcr24* and generates 24S,25-epoxycholesterol. In addition, the expression of Cyp46a1, cholesterol 24-hydroxylase, is low in fetal mouse. What then might be the consequence of high levels of 24S,25-epoxycholesterol in newborn brain? 24S,25-epoxycholesterol is an LXR ligand, and LXR ligands promote neurogenesis in developing brain (58). Thus, it seems possible that this oxysterol, which is particularly abundant in brain, is important for neurogenesis, and indicates yet another important function of an active mevalonate pathway. In addition, 24S,25-epoxycholesterol is a ligand to Insig and may be involved in the fine-tuning of acute cholesterol homeostasis.

Desmosterol is particularly abundant in the fetus and newborn animal (4, 54), in part because of the low expression of *Dhcr24*, as discussed above. This leads to the possibility of oxysterol formation using this substrate. This has been shown to be possible both in vitro and in vivo (30, 52). Here, we show that oxysterols derived from desmosterol are present in newborn mouse brain, with hydroxylation occurring in both the steroid nucleus and side-chain. Desmosterol, unlike its 26-hydroxy metabolites, is also an LXR ligand (52, 56), and here, we show that it is a ligand to both the α and β isoforms of the receptor in a neural cell line. From the present study, it is impossible to determine the relative importance of the LXR ligands found in newborn brain. Although desmosterol is present in far greater abundance than 24S,25-epoxycholesterol, or any other LXR ligand, it is likely that the majority is trapped in cell membranes and unavailable to act as a signaling molecule. On the other hand, the greater cytoplasmic solubility makes 24S,25-epoxycholesterol a better candidate as a active LXR ligand in newborn brain.

REFERENCES

1. Dietschy, J. M., and S. D. Turley. 2004. Thematic review series: brain lipids. Cholesterol metabolism in the central nervous system during early development and in the mature animal. *J. Lipid Res.* **45:** 1375–1397.
2. Björkhem, I., and S. Meaney. 2004. Brain cholesterol: long secret life behind a barrier. *Arterioscler. Thromb. Vasc. Biol.* **24:** 806–815.
3. Dietschy, J. M., and S. D. Turley. 2001. Cholesterol metabolism in the brain. *Curr. Opin. Lipidol.* **12:** 105–112.
4. Tint, G. S., H. Yu, Q. Shang, G. Xu, and S. B. Patel. 2006. The use of the Dhcr7 knockout mouse to accurately determine the origin of fetal sterols. *J. Lipid Res.* **47:** 1535–1541.
5. Wang, Y., K. M. Sousa, K. Bodin, S. Theofilopoulos, P. Sacchetti, M. Hornshaw, G. Woffendin, K. Karu, J. Sjövall, E. Arenas, et al. 2009. Targeted lipidomic analysis of oxysterols in the embryonic central nervous system. *Mol. Biosyst.* **5:** 529–541.
6. Xie, C., E. G. Lund, S. D. Turley, D. W. Russell, and J. M. Dietschy. 2003. Quantitation of two pathways for cholesterol excretion from the brain in normal mice and mice with neurodegeneration. *J. Lipid Res.* **44:** 1780–1789.
7. Lütjohann, D., O. Breuer, G. Ahlborg, I. Nennesmo, A. Siden, U. Diczfalusy, and I. Björkhem. 1996. Cholesterol homeostasis in human brain: evidence for an age-dependent flux of 24S-hydroxycholesterol from the brain into the circulation. *Proc. Natl. Acad. Sci. USA.* **93:** 9799–9804.
8. Lund, E. G., J. M. Guileyardo, and D. W. Russell. 1999. cDNA cloning of cholesterol 24-hydroxylase, a mediator of cholesterol homeostasis in the brain. *Proc. Natl. Acad. Sci. USA.* **96:** 7238–7243.
9. Ohyama, Y., S. Meaney, M. Heverin, L. Ekström, A. Brafman, M. Shafir, U. Andersson, M. Olin, G. Eggertsen, U. Diczfalusy, et al. 2006. Studies on the transcriptional regulation of cholesterol 24-hydroxylase (CYP46A1): marked insensitivity toward different regulatory axes. *J. Biol. Chem.* **281:** 3810–3820.
10. Janowski, B. A., M. J. Grogan, S. A. Jones, G. B. Wisely, S. A. Kliewer, E. J. Corey, and D. J. Mangelsdorf. 1999. Structural requirements of ligands for the oxysterol liver X receptors LXRalpha and LXRbeta. *Proc. Natl. Acad. Sci. USA.* **96:** 266–271.
11. Lehmann, J. M., S. A. Kliewer, L. B. Moore, T. A. Smith-Oliver, B. B. Oliver, J. L. Su, S. S. Sundseth, D. A. Winegar, D. E. Blanchard, T. A. Spencer, et al. 1997. Activation of the nuclear receptor LXR by oxysterols defines a new hormone response pathway. *J. Biol. Chem.* **272:** 3137–3140.
12. Mellon, S. H., and L. D. Griffin. 2002. Neurosteroids: biochemistry and clinical significance. *Trends Endocrinol. Metab.* **13:** 35–43.
13. Yao, Z. X., R. C. Brown, G. Teper, J. Greeson, and V. Papadopoulos. 2002. 22R-hydroxycholesterol protects neuronal cells from beta-amyloid-induced cytotoxicity by binding to beta-amyloid peptide. *J. Neurochem.* **83:** 1110–1119.
14. Koldamova, R. P., I. M. Lefterov, M. D. Ikonomovic, J. Skoko, P. I. Lefterov, B. A. Isanski, S. T. DeKosky, and J. S. Lazo. 2003. 22R-hydroxycholesterol and 9-cis-retinoic acid induce ATP-binding cassette transporter A1 expression and cholesterol efflux in brain cells and decrease amyloid beta secretion. *J. Biol. Chem.* **278:** 13244–13256.
15. Radhakrishnan, A., Y. Ikeda, H. J. Kwon, M. S. Brown, and J. L. Goldstein. 2007. Sterol-regulated transport of SREBPs from endoplasmic reticulum to Golgi: oxysterols block transport by binding to Insig. *Proc. Natl. Acad. Sci. USA.* **104:** 6511–6518.
16. Horton, J. D., J. L. Goldstein, and M. S. Brown. 2002. SREBPs: activators of the complete program of cholesterol and fatty acid synthesis in the liver. *J. Clin. Invest.* **109:** 1125–1131.
17. Brown, M. S., and J. L. Goldstein. 2009. Cholesterol feedback: from Schoenheimer's bottle to Scap's MELADL. *J. Lipid Res.* **50 (Suppl):** S15–S27.
18. Wong, J., C. M. Quinn, I. C. Gelissen, and A. J. Brown. 2008. Endogenous 24(S),25-epoxycholesterol fine-tunes acute control of cellular cholesterol homeostasis. *J. Biol. Chem.* **283:** 700–707.
19. Liere, P., A. Pianos, B. Eychenne, A. Cambourg, K. Bodin, W. Griffiths, M. Schumacher, E. E. Baulieu, and J. Sjövall. 2009. Analysis of pregnenolone and dehydroepiandrosterone in rodent brain: cholesterol autoxidation is the key. *J. Lipid Res.* **50:** 2430–2444.
20. Schroepfer, G. J., Jr. 2000. Oxysterols: modulators of cholesterol metabolism and other processes. *Physiol. Rev.* **80:** 361–554.
21. Heverin, M., N. Bogdanovic, D. Lütjohann, T. Bayer, I. Pikuleva, L. Bretillon, U. Diczfalusy, B. Winblad, and I. Björkhem. 2004. Changes in the levels of cerebral and extracerebral sterols in the brain of patients with Alzheimer's disease. *J. Lipid Res.* **45:** 186–193.
22. Karu, K., M. Hornshaw, G. Woffendin, K. Bodin, M. Hamberg, G. Alvelius, J. Sjövall, J. Turton, Y. Wang, and W. J. Griffiths. 2007. Liquid chromatography-mass spectrometry utilizing multi-stage fragmentation for the identification of oxysterols. *J. Lipid Res.* **48:** 976–987.
23. Liu, S., J. Sjövall, and W. J. Griffiths. 2003. Neurosteroids in rat brain: extraction, isolation, and analysis by nanoscale liquid chromatography-electrospray mass spectrometry. *Anal. Chem.* **75:** 5835–5846.
24. McDonald, J. G., B. M. Thompson, E. C. McCrum, and D. W. Russell. 2007. Extraction and analysis of sterols in biological matrices by

high performance liquid chromatography electrospray ionization mass spectrometry. *Methods Enzymol.* **432:** 145–170.

25. Griffiths, W. J., and Y. Wang. 2011. Analysis of oxysterol metabolomes. *Biochim. Biophys. Acta.* **1811:** 784–799.

26. Dzeletovic, S., O. Breuer, E. Lund, and U. Diczfalusy. 1995. Determination of cholesterol oxidation products in human plasma by isotope dilution-mass spectrometry. *Anal. Biochem.* **225:** 73–80.

27. Honda, A., K. Yamashita, T. Hara, T. Ikegami, T. Miyazaki, M. Shirai, G. Xu, M. Numazawa, and Y. Matsuzaki. 2009. Highly sensitive quantification of key regulatory oxysterols in biological samples by LC-ESI-MS/MS. *J. Lipid Res.* **50:** 350–357.

28. Karu, K., J. Turton, Y. Wang, and W. J. Griffiths. 2011. Nano-liquid chromatography-tandem mass spectrometry analysis of oxysterols in brain: monitoring of cholesterol autoxidation. *Chem. Phys. Lipids.* **164:** 411–424.

29. Griffiths, W. J., Y. Wang, G. Alvelius, S. Liu, K. Bodin, and J. Sjövall. 2006. Analysis of oxysterols by electrospray tandem mass spectrometry. *J. Am. Soc. Mass Spectrom.* **17:** 341–362.

30. Pikuleva, I., and N. B. Javitt. 2003. Novel sterols synthesized via the CYP27A1 metabolic pathway. *Arch. Biochem. Biophys.* **420:** 35–39.

31. Marcos, J., C. H. Shackleton, M. M. Buddhikot, F. D. Porter, and G. L. Watson. 2007. Cholesterol biosynthesis from birth to adulthood in a mouse model for 7-dehydrosterol reductase deficiency (Smith-Lemli-Opitz syndrome). *Steroids.* **72:** 802–808.

32. Ogundare, M., S. Theofilopoulos, A. Lockhart, L. J. Hall, E. Arenas, J. Sjövall, A. G. Brenton, Y. Wang, and W. J. Griffiths. 2010. Cerebrospinal fluid steroidomics: are bioactive bile acids present in brain? *J. Biol. Chem.* **285:** 4666–4679.

33. MacLachlan, J., A. T. Wotherspoon, R. O. Ansell, and C. J. Brooks. 2000. Cholesterol oxidase: sources, physical properties and analytical applications. *J. Steroid Biochem. Mol. Biol.* **72:** 169–195.

34. Shackleton, C. H., H. Chuang, J. Kim, X. de la Torre, and J. Segura. 1997. Electrospray mass spectrometry of testosterone esters: potential for use in doping control. *Steroids.* **62:** 523–529.

35. Lütjohann, D., A. Brzezinka, E. Barth, D. Abramowski, M. Staufenbiel, K. von Bergmann, K. Beyreuther, G. Multhaup, and T. A. Bayer. 2002. Profile of cholesterol-related sterols in aged amyloid precursor protein transgenic mouse brain. *J. Lipid Res.* **43:** 1078–1085.

36. Griffiths, W. J., and Y. Wang. 2009. Sterol lipidomics in health and disease: methodologies and applications. *Eur. J. Lipid Sci. Technol.* **111:** 14–38.

37. Lütjohann, D., I. Björkhem, S. Locatelli, C. Dame, J. Schmolling, K. von Bergmann, and H. Fahnenstich. 2001. Cholesterol dynamics in the foetal and neonatal brain as reflected by circulatory levels of 24S-hydroxycholesterol. *Acta Paediatr.* **90:** 652–657.

38. Lund, E. G., T. A. Kerr, J. Sakai, W. P. Li, and D. W. Russell. 1998. cDNA cloning of mouse and human cholesterol 25-hydroxylases, polytopic membrane proteins that synthesize a potent oxysterol regulator of lipid metabolism. *J. Biol. Chem.* **273:** 34316–34327.

39. Mast, N., R. Norcross, U. Andersson, M. Shou, K. Nakayama, I. Björkhem, and I. A. Pikuleva. 2003. Broad substrate specificity of human cytochrome P450 46A1 which initiates cholesterol degradation in the brain. *Biochemistry.* **42:** 14284–14292.

40. Cali, J. J., and D. W. Russell. 1991. Characterization of human sterol 27-hydroxylase. A mitochondrial cytochrome P-450 that catalyzes multiple oxidation reaction in bile acid biosynthesis. *J. Biol. Chem.* **266:** 7774–7778.

41. Repa, J. J., E. G. Lund, J. D. Horton, E. Leitersdorf, D. W. Russell, J. M. Dietschy, and S. D. Turley. 2000. Disruption of the sterol 27-hydroxylase gene in mice results in hepatomegaly and hypertriglyceridemia. Reversal by cholic acid feeding. *J. Biol. Chem.* **275:** 39685–39692.

42. Lund, E., I. Björkhem, C. Furster, and K. Wikvall. 1993. 24-, 25- and 27-hydroxylation of cholesterol by a purified preparation of 27-hydroxylase from pig liver. *Biochim. Biophys. Acta.* **1166:** 177–182.

43. Lund, E. G., C. Xie, T. Kotti, S. D. Turley, J. M. Dietschy, and D. W. Russell. 2003. Knockout of the cholesterol 24-hydroxylase gene in mice reveals a brain-specific mechanism of cholesterol turnover. *J. Biol. Chem.* **278:** 22980–22988.

44. Compagnone, N. A., A. Bulfone, J. L. Rubenstein, and S. H. Mellon. 1995. Expression of the steroidogenic enzyme P450scc in the central and peripheral nervous systems during rodent embryogenesis. *Endocrinology.* **136:** 2689–2696.

45. Jelinek, D. F., S. Andersson, C. A. Slaughter, and D. W. Russell. 1990. Cloning and regulation of cholesterol 7 alpha-hydroxylase, the rate-limiting enzyme in bile acid biosynthesis. *J. Biol. Chem.* **265:** 8190–8197.

46. Murphy, R. C., and K. M. Johnson. 2008. Cholesterol, reactive oxygen species, and the formation of biologically active mediators. *J. Biol. Chem.* **283:** 15521–15525.

47. Fahy, E., S. Subramaniam, H. A. Brown, C. K. Glass, A. H. Merrill, Jr., R. C. Murphy, C. R. Raetz, D. W. Russell, Y. Seyama, W. Shaw, et al. 2005. A comprehensive classification system for lipids. *J. Lipid Res.* **46:** 839–861.

48. Byon, C. Y., and M. Gut. 1980. Steric considerations regarding the biodegradation of cholesterol to pregnenolone. Exclusion of (22S)-22-hydroxycholesterol and 22-ketocholesterol as intermediates. *Biochem. Biophys. Res. Commun.* **94:** 549–552.

49. Kautsky, G. J., C. Bouboulis, R. Becker, and C. King. 1958. Synthesis and metabolism of 22-ketocholesterol-23-C14. *J. Biol. Chem.* **233:** 1340–1342.

50. Karlaganis, G., and J. Sjövall. 1984. Formation and metabolism of bile alcohols in man. *Hepatology.* **4:** 966–973.

51. Shefer, S., F. W. Cheng, B. Dayal, S. Hauser, G. S. Tint, G. Salen, and E. H. Mosbach. 1976. A 25-hydroxylation pathway of cholic acid biosynthesis in man and rat. *J. Clin. Invest.* **57:** 897–903.

52. Heverin, M., S. Meaney, A. Brafman, M. Shafir, M. Olin, M. Shafaati, S. von Bahr, L. Larsson, A. Lövgren-Sandblom, U. Diczfalusy, et al. 2007. Studies on the cholesterol-free mouse: strong activation of LXR-regulated hepatic genes when replacing cholesterol with desmosterol. *Arterioscler. Thromb. Vasc. Biol.* **27:** 2191–2197.

53. McDonald, J. G., D. D. Smith, A. R. Stiles, and D. W. Russell. 2012. A comprehensive method for extraction and quantitative analysis of sterols and secosteroids from human plasma. *J. Lipid Res.* **53:** 1399–1409.

54. Quan, G., C. Xie, J. M. Dietschy, and S. D. Turley. 2003. Ontogenesis and regulation of cholesterol metabolism in the central nervous system of the mouse. *Brain Res. Dev. Brain Res.* **146:** 87–98.

55. Rodríguez-Acebes, S., P. de la Cueva, C. Fernandez-Hernando, A. J. Ferruelo, M. A. Lasuncion, R. B. Rawson, J. Martinez-Botas, and D. Gomez-Coronado. 2009. Desmosterol can replace cholesterol in sustaining cell proliferation and regulating the SREBP pathway in a sterol-Delta24-reductase-deficient cell line. *Biochem. J.* **420:** 305–315.

56. Yang, C., J. G. McDonald, A. Patel, Y. Zhang, M. Umetani, F. Xu, E. J. Westover, D. F. Covey, D. J. Mangelsdorf, J. C. Cohen, et al. 2006. Sterol intermediates from cholesterol biosynthetic pathway as liver X receptor ligands. *J. Biol. Chem.* **281:** 27816–27826.

57. Roberg-Larsen, H., M. F. Strand, A. Grimsmo, P. A. Olsen, J. L. Dembinski, F. Rise, E. Lundanes, T. Greibrokk, S. Krauss, and S. R. Wilson. 2012. High sensitivity measurements of active oxysterols with automated filtration/filter backflush-solid phase extraction-liquid chromatography-mass spectrometry. *J. Chromatogr. A.* **1255:** 291–297.

58. Sacchetti, P., K. M. Sousa, A. C. Hall, I. Liste, K. R. Steffensen, S. Theofilopoulos, C. L. Parish, C. Hazenberg, L. A. Richter, O. Hovatta, et al. 2009. Liver X receptors and oxysterols promote ventral midbrain neurogenesis in vivo and in human embryonic stem cells. *Cell Stem Cell.* **5:** 409–419.

59. Wang, L., G. U. Schuster, K. Hultenby, Q. Zhang, S. Andersson, and J. A. Gustafsson. 2002. Liver X receptors in the central nervous system: from lipid homeostasis to neuronal degeneration. *Proc. Natl. Acad. Sci. USA.* **99:** 13878–13883.

60. Schumacher, M., P. Liere, Y. Akwa, K. Rajkowski, W. Griffiths, K. Bodin, J. Sjövall, and E. E. Baulieu. 2008. Pregnenolone sulfate in the brain: a controversial neurosteroid. *Neurochem. Int.* **52:** 522–540.

61. Saijo, K., J. G. Collier, A. C. Li, J. A. Katzenellenbogen, and C. K. Glass. 2011. An ADIOL-ERbeta-CtBP transrepression pathway negatively regulates microglia-mediated inflammation. *Cell.* **145:** 584–595.